Effect of Microalloying with Silicon on High Temperature Oxidation Resistance of Novel Refractory High-Entropy Alloy Ta-Mo-Cr-Ti-Al

Franz Mueller[a], Bronislava Gorr[a], Hans-Juergen Christ[a], Hans Chen[b], Alexander Kauffmann[b], Martin Heilmaier[b]

[a]Institut für Werkstofftechnik, Universität Siegen, Siegen, GERMANY

[b]Institut für Angewandte Materialien, Karlsruher Institut für Technologie (KIT),Karlsruhe, GERMANY

F.Mueller

Institut für Werkstofftechnik, Universität Siegen, Paul-Bonatz-Strasse 9-11, 57068 Siegen (GERMANY)

Email: franz.mueller@uni-siegen.de

Effect of Microalloying with Silicon on High Temperature Oxidation Resistance of Novel Refractory High-Entropy Alloy Ta-Mo-Cr-Ti-Al

The effect of 1 at.% Si addition to the refractory high-entropy alloy (HEA) Ta-Mo-Cr-Ti-Al on the high temperature oxidation resistance in air between 900 °C and 1100 °C was studied. Due to the formation of protective chromia-rich and alumina scales, the thermogravimetric curves for Ta-Mo-Cr-Ti-Al and Ta-Mo-Cr-Ti-Al-1Si showed small mass changes and low oxidation rates which are on the level of chromia-forming alloys. The oxide scales formed on both alloys at all temperatures are complex and consist of outermost TiO_2, intermediate Al_2O_3, and (Cr,Ta,Ti)-rich oxide at the interface oxide/substrate. The Si addition had a slightly detrimental effect on the oxidation resistance at all temperatures primarily as a result of increased internal corrosion attack observed in the Si-containing HEA. Large Laves phase particles distinctly found in the Si-containing alloy were identified to be responsible for the more rapid internal corrosion.

Keywords: High-entropy alloys; silicon effect; refractory metals; Laves phase; internal corrosion; high-temperature corrosion

Introduction

High-Entropy Alloys (HEAs) represent a novel class of multicomponent alloys which have drawn increasing attention among the material scientists worldwide because of a new attractive and simple concept of alloy design giving rise to unique properties of some HEAs [1-3]. In general, HEAs consist of at least 5 elements in equal or near-equal concentrations. From a thermodynamic point of view, HEAs should exhibit much larger mixing entropies than conventional alloys which may result in suppression of the formation of ordered intermetallic compounds, hence, promoting the formation of single-phase solid solutions with simple crystal structures [1]. However, experimental studies on numerous HEAs revealed that most of them do not show a single phase microstructure, rather intermetallic ordered phases such as like Laves, Sigma or higher

ordered B2 phases form in addition to the disordered solid solutions [4, 5]. In this case, according to Senkov [5], the term multi-principal element alloys (MPEA) may be more appropriate. Such two-phase alloys often show more interesting properties compared to those of the single-phase HEAs. For example, many refractory HEAs, which have been designed for high temperature structural applications and indeed show remarkable high temperature strength, also exhibit a multi-phase microstructure. Senkov et al. reported on two refractory HEAs Nb-Cr-Ti-Zr and Nb-V-Cr-Ti-Zr which consist of a disordered body-centered cubic (bcc) and an ordered C15 Laves phase. These alloys offer attractive properties as they exhibit high hardness due to the formation of the Laves phase accompanied by a favourably low density [6]. Another alloy system on basis of Al-Mo-Nb-Ta-Ti-Zr was found to form either a single-phase disordered cubic bcc crystal structure or a two-phase microstructure including the coherent ordered B2 phase [7]. Interestingly, the alloy with the coherent two-phase bcc/B2 microstructure Al-$Mo_{0.5}$-Nb-$Ta_{0.5}$-Ti-Zr exhibits a very high yield strength which is even superior to that of Ni-based superalloys in the temperature range from 20°C to 1200°C [8]. Our own studies on the equiatomic alloy Nb-Mo-Cr-Ti-Al showed that the alloy microstructure after the heat treatment at 1300°C consists of a disordered bcc-matrix and a small amount (< 0.5 vol.%) of Cr_2Nb Laves phase (C14, hexagonal) located predominately at the grain boundaries. Compression tests conducted at various temperatures showed relatively high yield strength up to 800 °C and an increasing ductility with increasing test temperature [9]. At temperatures up to approximately 400°C, the alloy, however, exhibits brittle behaviour. It was, though, found by hardness indentations in the grain interior that the bcc-matrix is plastically deformable and the alloy brittleness at low temperatures can be attributed to the presence of the Laves phase.

Although many refractory HEAs show outstanding mechanical properties [8], they

usually possess moderate high temperature corrosion resistance due to the formation of thick, complex, non-protective or volatile oxides. Senkov et al. investigated the oxidation behaviour of the refractory HEA Nb-Cr-Mo$_{0.5}$-Ta$_{0.5}$-Ti-Zr at 1000°C in air and found moderate oxidation resistance with nearly parabolic oxidation rates. The evaporation of molybdenum oxide leads to the formation of pores in one of the two bcc matrix phases. Further, cracks formed during oxidation in the regions of the Laves phase were observed [10]. By contrast, our own studies on the high temperature oxidation of Nb-Mo-Cr-Ti-Al between 900°C-1100°C in air showed linear oxidation rates and the formation of predominantly thick, non-protective oxide scales consisting of a mixed rutile solid solution phase [11]. In the very recent study, the beneficial effect of 1 at.% silicon addition to the refractory HEA Nb-Mo-Cr-Ti-Al on the oxidation resistance at 900°C-1000 °C was found [11].

Minor additions of silicon, which do not lead to the formation of brittle silicides, are, in general, beneficial in terms of the formation of protective oxide layers [12-15]. The most accepted theories on the Si effect on the oxidation behavior of chromia forming alloys are – depending on the alloy system – (i) the formation of a protective silica scale on the phase boundary substrate/oxide [16, 17] and (ii) the promotion of the development of a protective chromia layer, triggered by SiO$_2$ nucleation sites [18-20]. Bhowmik et al. investigated the effect of silicon additions to Cr-Cr$_2$Ta-based alloys, which consisted of a eutectic of Cr-based solid solution and the Cr$_2$Ta Laves phases with hexagonal C14 and C36 polymorph [12]. There, it was found that silicon additions of up to 7 at.% clearly improve the oxidation characteristics at 1000 °C and 1100 °C. Further, the silicon addition proofed to be beneficial for the fracture toughness by reducing the extent of internal nitridation [12].

In the present study, the oxidation behaviour of two refractory HEAs Ta-Mo-Cr-Ti-Al

and Ta-Mo-Cr-Ti-Al-1Si at temperatures between 900°C-1100°C in air is comparatively investigated in order to understand the impact of a minor Si addition on the oxidation resistance. Specifically, a mechanism-based consideration will be carried out comparing the results obtained with the positive effect of Si observed on the oxidation behaviour in the equiatomic alloy Nb-Mo-Cr-Ti-Al [11].

Experimental Procedures

The alloys were cast from elemental bulk material by arc-melting (arc-melter AM 0.5 by Edmund Bühler GmbH) in ~0.6 atm. of argon. The purities of the used elemental bulk materials Ta and Mo were 99.9%, while Cr, Ti, Al, Si had purities of 99 %, 99.8%, 99.9% and 99.9999%, respectively. The prepared buttons were flipped over and remelted at least five times in a water-chilled copper mold to facilitate alloy homogenization. The alloys were subsequently heat-treated at 1400 °C for 20 h in inert atmosphere. The ingots were then cut by electrical discharge machining (EDM) to dimensions of approximately 5 mm x 5 mm x 2 mm, polished up to 1200 grit and ultrasonically cleaned in ethanol directly before high-temperature exposure. The oxidation tests were carried out in a Rubotherm thermogravimetric system under isothermal conditions in laboratory air. To analyse the oxide morphology, a Focused Ion Beam - Scanning Electron Microscope (FIB-SEM) DualBeam system of type FEI Helios Nanolab 600 in combination with backscatter electron (BSE) imaging and energy dispersive X-ray spectroscopy (EDX) as well as electron backscatter diffraction (EBSD) was used. The composition of the oxide scales was analysed by X-ray diffraction (XRD) on oxidized samples. The XRD measurements were carried out using a X'Pert Pro MPD diffractometer operating in Bragg-Brentano geometry as described in Ref. [11].

Results

The overall compositions of the refractory high-entropy alloys are 20Ta-20Mo-20Cr-20Ti-20Al and 19.8Ta-19.8Mo-19.8Cr-19.8Ti-19.8Al-1Si (in at. %). After arc melting and homogenization at 1400°C for 20 hours both HEAs still show a multi-phase microstructure, i.e. an alloy matrix and Laves phases rich in Cr, Ta and Al as can be seen in Fig. 1 a) and b). Additional analyses using XRD (see. Fig. 2), EBSD and TEM (not shown here) revealed three modifications of Laves phase, i.e. hexagonal C14, cubic C15 and hexagonal C36, distributed in the matrix which consists of a bcc/B2 microstructure. While the relatively small particles of the Laves phase form preferably at the grain boundaries in the Si-free alloy, the particles of the Laves phase in the Si-containing HEA are significantly bigger and homogeneously distributed in the alloy matrix.
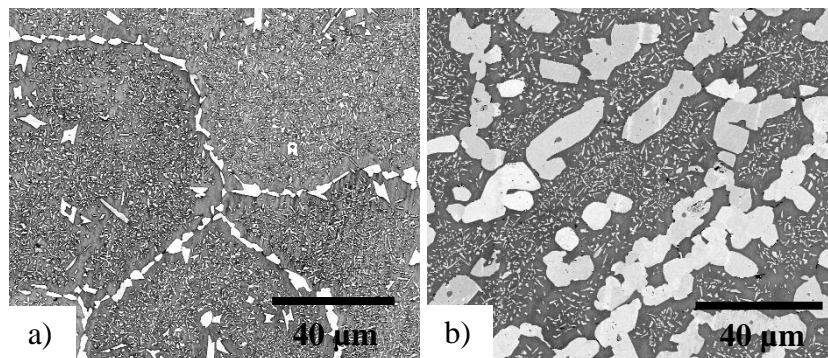

Figure 1. Backscattered electron micrographs of the substrate of a) Ta-Mo-Cr-Ti-Al and b) Ta-Mo-Cr-Ti-Al-1Si after heat treatment at 1400°C for 20h.
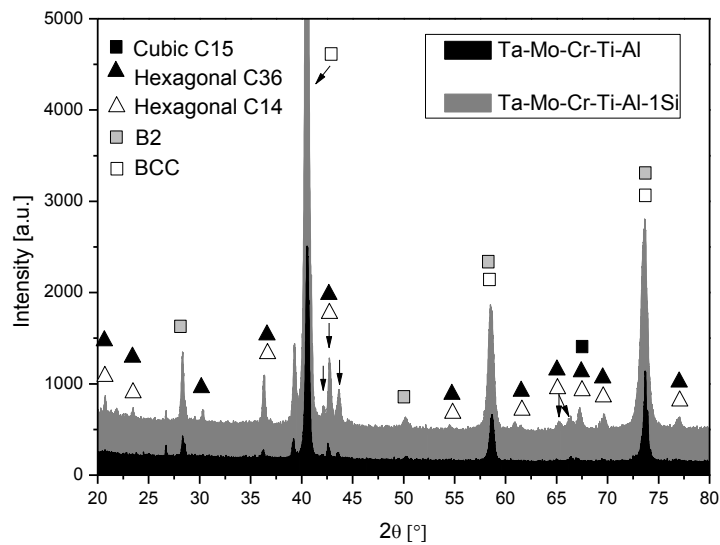
Figure 2. Results of the XRD analyses of alloys Ta-Mo-Cr-Ti-Al and Ta-Mo-Cr-Ti-Al-1Si after heat treatment at 1400°C for 20h.

The oxidation kinetics of the alloys Ta-Mo-Cr-Ti-Al and Ta-Mo-Cr-Ti-Al-1Si at 900 °C, 1000°C and 1100 °C in air is shown in Fig. 3a), b) and c) in double-linear representation. In order to determine whether the thermogravimetric curves obey a linear or a parabolic rate law, the square of the mass change versus time is plotted in Fig.3 d), e) and f). The oxidation curves between 900°C-1000°C obviously obey the parabolic rate law after a short period of transient oxidation indicating that the growth of the oxide scale proceeds through solid-state diffusion. At 1100°C, parabolic oxidation behaviour was only observed for Ta-Mo-Cr-Ti-Al whereas the Si-containing alloy exhibits increasing oxidation rates after 30 h of exposure. Although both alloys show generally relatively small mass changes and low oxidation rates at all temperatures, Ta-Mo-Cr-Ti-Al-1Si obviously possesses a lower oxidation resistance than the alloy Ta-Mo-Cr-Ti-Al.
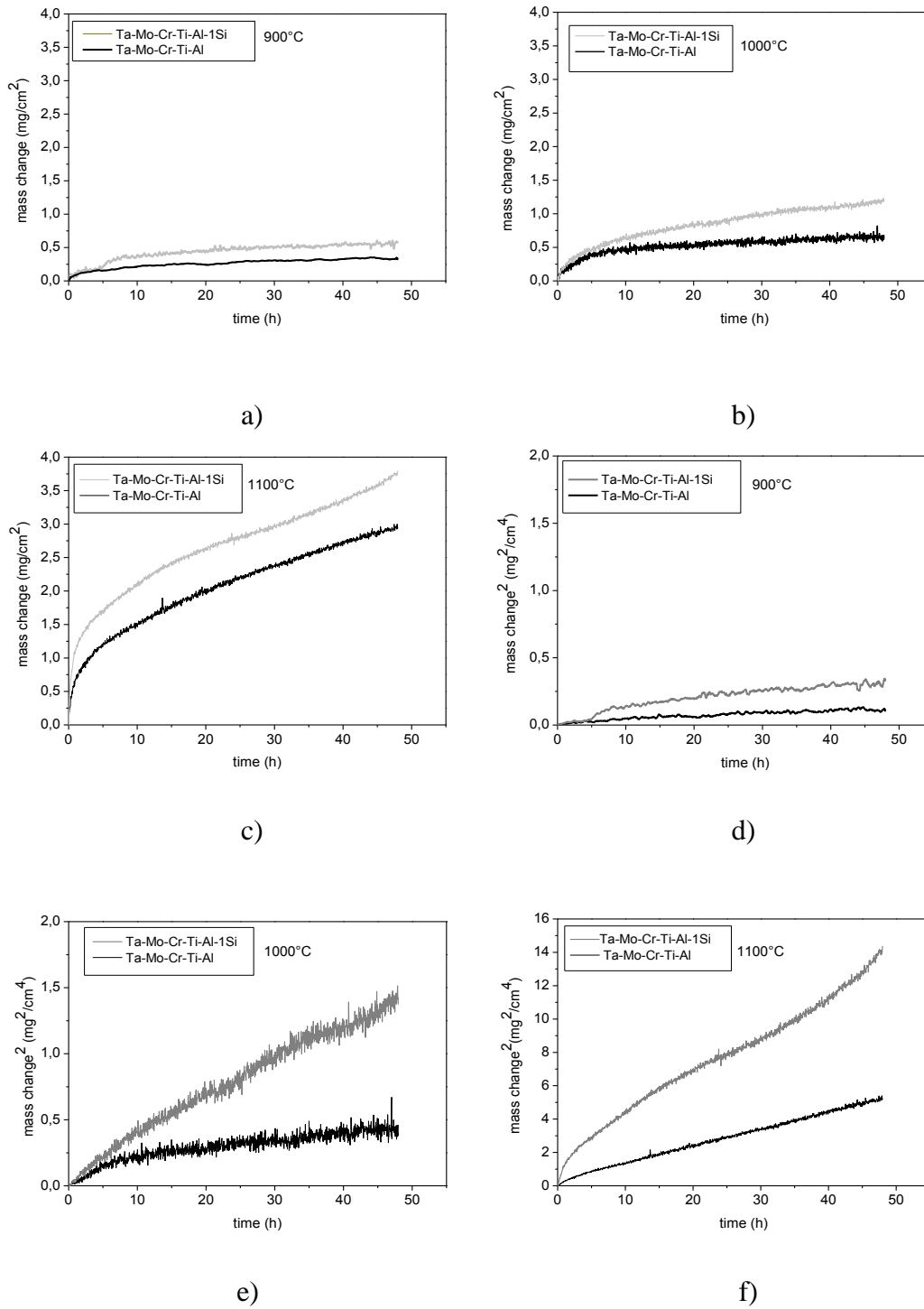
Figure 3. Thermogravimetric curves of Ta -Mo-Cr-Ti-Al with and without 1 at.% Si addition conducted during exposure in air at a) 900 °C, b) 1000 °C, c) 1100 °C; corresponding plots of the square of mass change versus oxidation time at d) 900 °C, e) 1000 °C and f) 1100 °C.

Microstructural SEM examination supplemented by EDX analyses of the oxidized samples after 48h of exposure at 900°C and 1000°C shows for both alloys the formation of rather similar oxide scales. Thus, the BSE micrographs of both alloys after 48 h of exposure at 1000°C are exemplarily displayed in Fig.4 to illustrate the general oxide scale morphologies that are also typical of oxides layers formed at 900°C. Figure 4 shows that both alloys form alumina layers underneath coarse Ti oxides. Below the alumina scale, a mixture of Cr-, Ti- and Ta-rich oxides was detected for both alloys. XRD measurements suggest the formation of TiO_2, Cr_2O_3, Al_2O_3 and $CrTaO_4$ in the oxide scale after 48 h of air exposure at 1000 °C for both alloys (see Fig. 5).

To determine the average thicknesses of the oxide scales formed on both alloys after 48 h of exposure at 900°C, 1000°C and 1100°C, several cross-section micrographs were used in each of which 20 individual measurements were carried out (see Table 1). In general, the oxide scale thicknesses increase with increasing temperatures, which corresponds to the thermogravimetric results. It was also found that the oxide scales of Ta-Mo-Cr-Ti-Al are generally more homogeneous with very little thickness variation, whereas Ta-Mo-Cr-Ti-Al-1Si formed both thick and thin oxide scales. Especially at 1100°C, Ta-Mo-Cr-Ti-Al-1Si displayed strong thickness variations depending on the location of measurement.

Table 1. Thicknesses of oxide scales formed on Ta-Mo-Cr-Ti-Al and Ta-Mo-Cr-Ti-Al-1Si after 48 h of exposure at 900°C, 1000°C and 1100°C in air.

	Oxide scale thicknesses after 48h of exposure (µm)		
Alloy	900°C	1000°C	1100°C
Ta-Mo-Cr-Ti-Al	1.2-1.3	4.9-5.0	7.9-9.3
Ta-Mo-Cr-Ti-Al-1Si	1.3-1.9	3.7-5.6	9.2-16.3

Underneath the oxide scales, a pronounced zone of internal corrosion in the matrix is found in both alloys at all temperatures. Appreciably oxidized phase boundaries between the Mo/Ta-rich bcc solid-solution matrix and the Laves phase (see Fig. 4b) were observed in the alloy Ta-Mo-Cr-Ti-Al-1Si, in particular in the vicinity of the large Laves phase particles, see Fig. 1b.
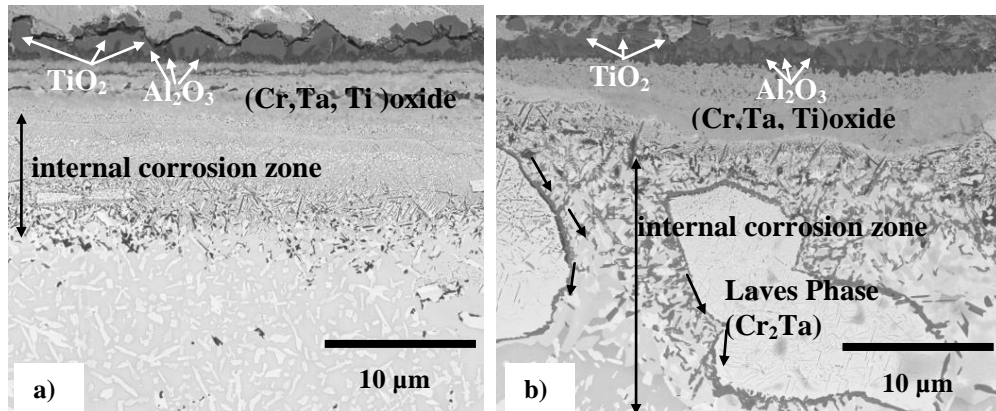

Figure 4. BSE cross-section images of oxidized (48 h, 1000 °C, air) samples of (a) Ta-Mo-Cr-Ti-Al , (b) Ta-Mo-Cr-Ti-Al-1Si. Oxidized phase boundaries between matrix and the Laves phase grains are marked with dark arrows.

The oxide scales formed on alloys studied at 1100°C are, in fact, very similar to those formed at 1000°C, however, they revealed some particular features. Figure 6 shows micrographs of Ta-Mo-Cr-Ti-Al and Ta-Mo-Cr-Ti-Al-1Si after 48 h of exposure to air

at 1100°C. Obviously, the oxide scales are locally more buckled and, interestingly, this is even more pronounced in case of the alloy Ta-Mo-Cr-Ti-Al-1Si (see Fig. 6 b)). In addition, for Ta-Mo-Cr-Ti-Al-1Si one severely oxidized sample edge rich in Ta and partially in Cr was found (see Fig. 7).
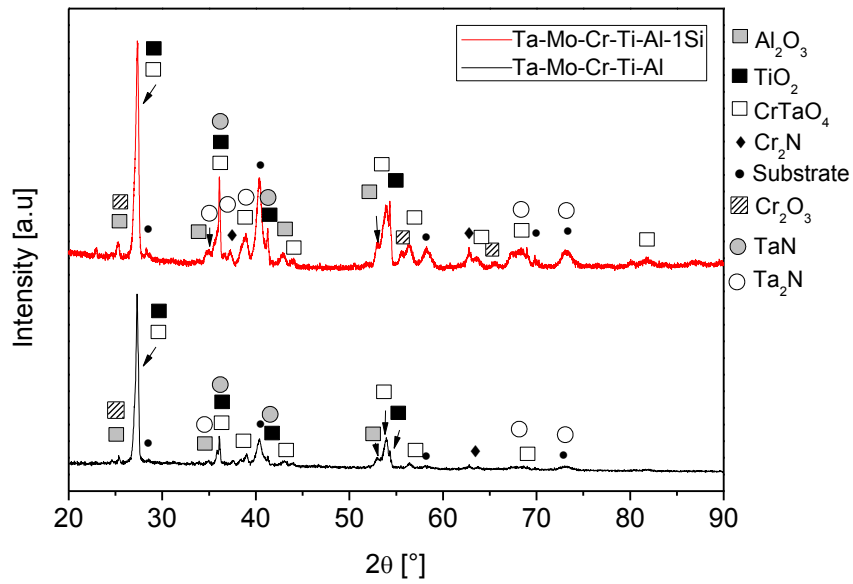

Figure 5. Results of the XRD analyses carried out on alloys Ta-Mo-Cr-Ti-Al and Ta-Mo-Cr-Ti-Al-1Si after 48h of exposure in air at 1000 °C.
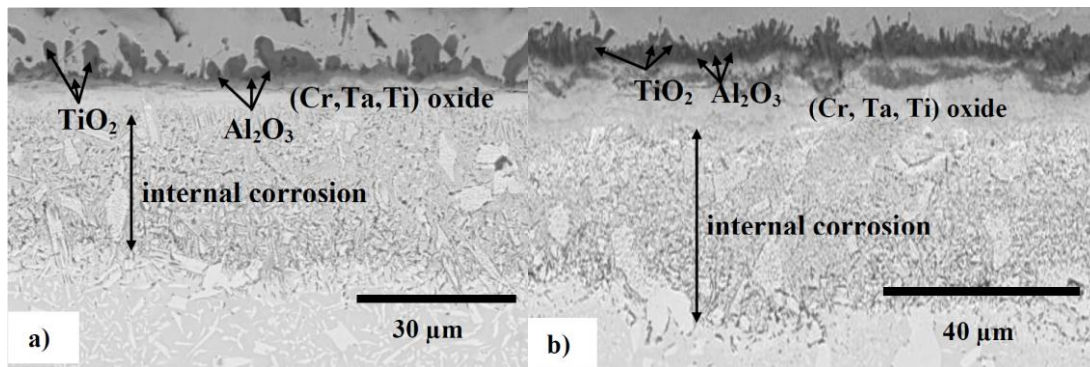

Figure 6. BSE images of a) Ta-Mo-Cr-Ti-Al and b) Ta-Mo-Cr-Ti-Al-1Si after 48 h of exposure in air at 1100 °C.
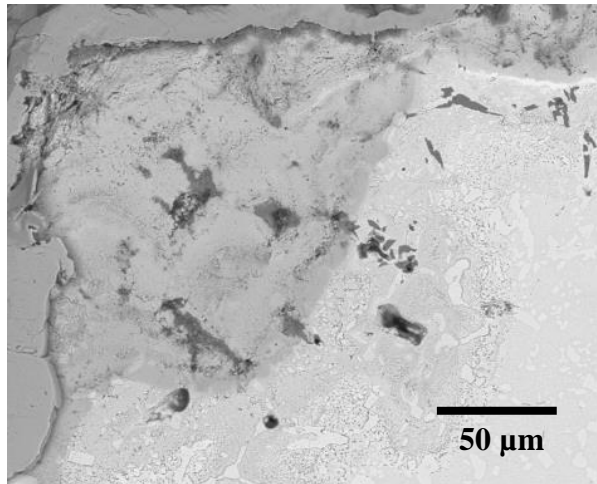
Figure 7. Example of a severely oxidized sample edge of Ta-Mo-Cr-Ti-Al-1Si after 48 h exposure in air at 1100°C.

As mentioned above, both alloys show a pronounced zone of internal corrosion with large precipitates enriched in Ta and Cr. XRD measurements after 48 h of exposure to air at 1000°C revealed the formation of several nitrides, i.e. TaN, Ta_2N and Cr_2N (see Fig. 5). Further EBSD measurements of the internal corrosion zones in both alloys documented even more corrosion products such as CrN, TiN, Cr_2O_3 and Al_2O_3. Figure 8 shows exemplarily results of the EBSD measurements of the internal corrosion zone in Ta-Mo-Cr-Ti-Al after 6 h of oxidation at 1000 °C in air. The results are in accordance with those obtained using XRD (see Fig.5). Interestingly, the appearance of the internal corrosion depends strongly on the size/shape and amount of the Laves phase (see Fig. 4). This means that the matrix near large Laves phase particles suffers from more severe inner corrosion attacks. The pronounced internal corrosion is already visible around the large Laves phase particles of Ta-Mo-Cr-Ti-Al-1Si after relatively short exposure time (6h) at 1000 °C (see Fig.9). Further, Fig. 9 clearly shows that the oxide scale formed on top of the Laves phase is much thinner and more protective than that formed on top of the matrix phase. EDX scans of oxide scales formed on top of Laves phase particles after 48 h of oxidation at 1000 °C (not shown here) further yield the formation of Ta-

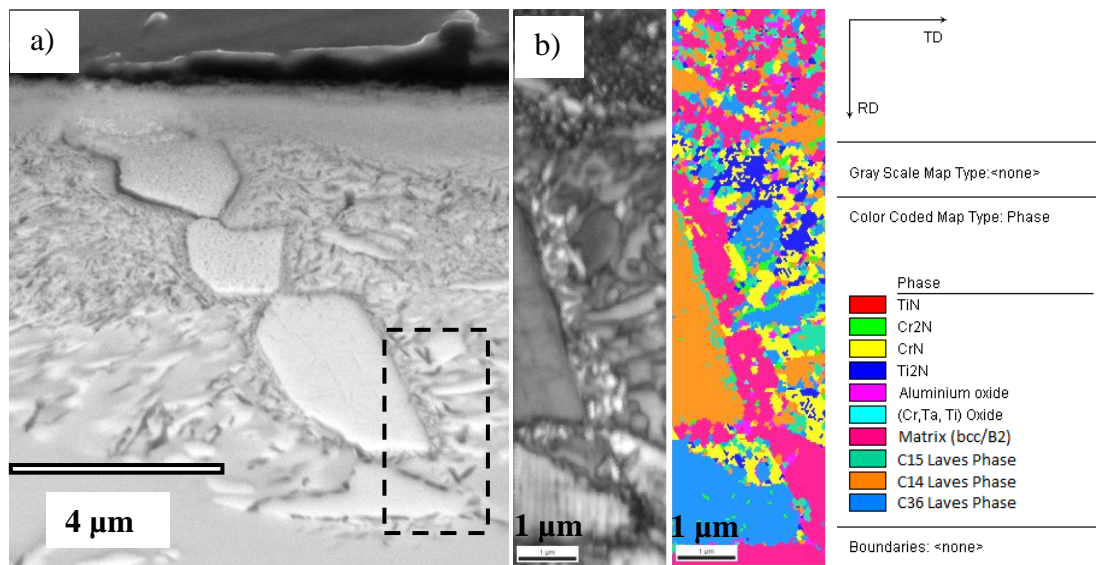rich oxides beneath a thin outermost layer of chromia.

Figure 8. a) BSE cross section image and b) EBSD analysis of the marked zone in a) after 6 h of exposure of the alloy Ta-Mo-Cr-Ti-Al at 1000 °C in air.
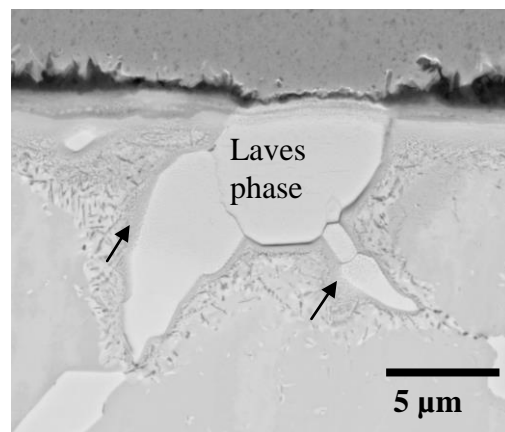

Figure 9. BSE micrographs of Ta-Mo-Cr-Ti-Al-1Si after 6 h of exposure in air at 1000 °C. Massive internal corrosion along the phase boundaries of the big Laves phase is indicated by arrows.

Discussion

The thermogravimetric measurements conducted during oxidation of the alloy Ta-Mo-Cr-Ti-Al-1Si show higher mass changes than those of the Si-free HEA at all temperatures. At 1100 °C, Ta-Mo-Cr-Ti-Al-1Si exhibits increasing oxidation kinetics after 30 h of exposure similar to break-away oxidation, while parabolic oxidation was

observed at lower temperatures. This strong increase in the oxidation kinetics can be attributed to the more pronounced internal corrosion in the vicinity of the Laves phase particles. Also, massive oxidation of one sample edge for Ta-Mo-Cr-Ti-Al-1Si after 48h of exposure at 1100°C in air occurred (see Fig. 7). The results of the TGA analyses correspond to those of the microstructural investigations: the oxide scales formed on the Si-containing alloys is slightly thicker compared to those formed on the Si-free alloy. Despite the high amount of highly reactive refractory elements, both alloys still exhibit good oxidation behaviour with small mass changes and low oxidation rates that are comparable with those of chromia and alumina forming alloys, respectively (see Fig. 10).
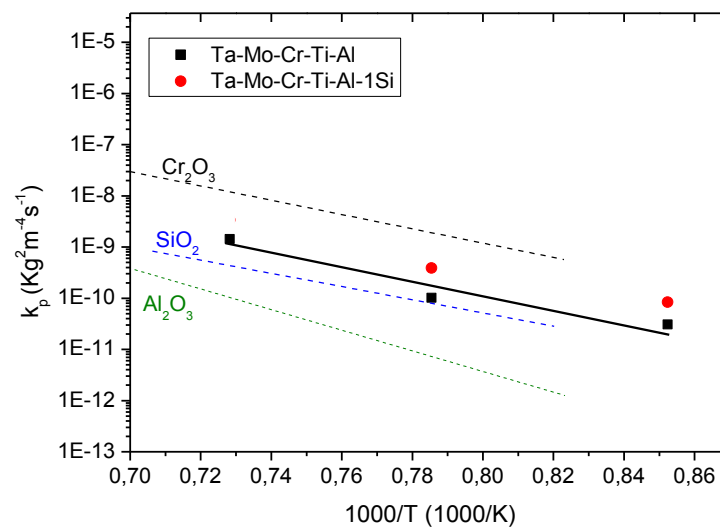
Figure 10. Overview of the parabolic rate constants for Ta-Mo-Cr-Ti-Al-(1Si) and Ni-based alloys [21].

The high oxidation resistance between 900°C-1000°C of both alloys can be explained by the formation of alumina- and chromia-rich layers among the complex oxide scales. In general, the corrosion process of both alloys in the initial stage of oxidation can be rationalized by the interplay between the oxidation of the bcc/B2 matrix leading to the

formation of a complex oxide scale including a protective alumina layer, the oxidation of the Laves phase resulting in the formation of a thin external chromia layer and the inner corrosion process causing the formation of nitrides CrN, Cr_2N, TiN and oxides, especially alumina (see Fig. 8). The severe formation of nitrides can apparently be attributed to the presence of the chromia scale. Chromia scales are generally permeable to nitrogen and the rapid formation of Cr_2N, which occurs at a faster rate than Cr_2O_3, has been one of the major obstacles to the practical use of Cr-based alloys in nitrogen containing environments [22]. It can therefore be assumed that nitrogen diffuses through the chromia scales formed on the Laves phase particles as well as through the phase boundaries between the matrix and the Laves phase.

To assess the formation of possible corrosion products, the standard free energies of formation of relevant oxides and nitrides were calculated at 1000 °C using the commercial software FactSage. The corresponding values for the oxides and the nitrides are listed in tables 2 and 3, respectively. Obviously TiO_2 and Al_2O_3 exhibit the lowest standard free energies. These compounds were found as external oxide scales as well as internally formed corrosion products. In terms of the thermodynamic stability, TiO_2 and also Al_2O_3 are followed by Ta_2O_5 and Cr_2O_3 (see table 2). This may imply that below the chromia scale that forms on the Laves phase at the initial stage of oxidation the partial pressure of oxygen is still high enough for the formation of Ta_2O_5. Further, Ta_2O_5 may then react with chromia to form the $CrTaO_4$ mixed oxide, which was observed in our study, according to the following reaction [23]:

$$Cr_2O_3 + Ta_2O_5 \rightarrow 2\ CrTaO_4$$
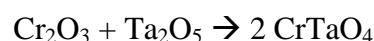
Moreover, since Ta_2O_5, TiO_2, $CrTaO_4$ and SiO_2 all form oxides with the rutile crystal structure, it is possible that these oxides may react with each other leading to the

formation of mixed rutile solid solutions after prolonged oxidation time. Tena et al. synthesized a rutile solid-solution $Cr_xTi_{1-2x}Ta_xO_2$ (0<x<0·5) by firing mixtures of Cr_2O_3, Ta_2O_5 and TiO_2 at 1300 °C. They found that $CrTaO_4$ formed as an intermediate rutile solid solution phase in samples synthesized by the oxide mixtures [24]. Also Joy et al. synthesized various mixed rutile solid solutions with the stoichiometry of M'$TiTaO_6$ (M'= Al, Cr, Fe) by mixing high purity of Ta_2O_5, TiO_2, Cr_2O_3 and Al_2O_3 in stoichiometric proportions and subsequent heating between 900 °C and 1200°C [25]. To confirm whether the formation of such oxide solid solutions takes place in refractory HEAs presented in this paper, further investigations after both, shorter and longer exposure times are needed.

As mentioned above, the zones of internal corrosion were observed in both alloys at all temperatures, whereas more pronounced internal corrosion was identified in the Si-containing alloy. Obviously, the effect of internal corrosion appears to be the more important factor than scaling. In fact, the more pronounced internal corrosion in the Si-containing alloy seems to account for the increased mass change for the Si-containing alloy. As mentioned above, especially the phase boundaries between the Laves phase particles and the matrix were susceptible to rapid and massive corrosion due to permeation of nitrogen through the thin chromia layer formed exclusively on the Laves phase. In addition, it is well-known that the diffusivity in phase- and grain boundaries is higher than in the bulk metal because the less closely packed atomic arrangement in the phase boundary offers faster diffusion paths. Laves phase, by contrast, exhibits complex and tightly-packed crystal structures with an overall packing density of 0.71 [26] which is even higher than the one in bcc/B2 (0.68) crystal structures. Thus, the Laves phases may exhibit lower oxygen/nitrogen permeability than the bcc/B2 matrix phase. For example, in the system Ti-Al-Cr, it was found that the (Cr,

Al)$_2$Ti Laves phase has a lower oxygen permeability than the hcp/bcc matrix phase and, thus, formed external alumina scales [27, 28]. Based on these considerations, one can suppose the following relationship of oxygen and nitrogen diffusivity in both alloys Ta-Mo-Cr-Ti-Al-(1Si): $D^0_{PB} > D^0_{bcc/B2} > D^0_{Laves\ phase}$. Here, D^0_{PB} denotes the oxygen and nitrogen diffusivity along phase boundaries. This assumption may explain the rapid corrosion of the phase boundaries between the matrix and the Laves phase (see Fig. 9). It should, however, be noted that the changes in the chemical compositions of the phases in the alloys may also affect the element activities influencing the diffusion processes in the alloy phases.

Laves phase remains, in contrary, largely unaffected by internal corrosion. As significantly more and larger particles of the Laves phase (and consequently more phase boundary area) are formed in the alloy Ta-Mo-Cr-Ti-Al-1Si (see Fig. 1), the internal corrosion attacks appear to be more severe than those in the Si-free alloy. It can, therefore, be concluded that the more pronounced internal corrosion, in addition to the slightly thicker oxide scales, can explain the higher mass change measured for the alloy Ta-Mo-Cr-Ti-Al-1Si during exposure in air at temperatures between 900°C and 1000°C compared to the Si-free alloy.

The reason why the silicon addition increases the volume fraction and the size of the Laves phase in Ta-Mo-Cr-Ti-Al-1Si is still unclear. Unfortunately, it was not possible for the present alloy system to determine the Si concentration in the different phases due to peak overlapping of Ta-M and Si-K peaks [29]. For binary Cr(Ta)-Cr$_2$Ta and Cr(Nb)-Cr$_2$Nb alloys, however, it was found that with increasing Si content, Si partitions heavily into the Laves phase by occupying Cr sub-lattice sites. Therefore, the volume fraction of the Laves phase was observed to increase substantially in these alloy systems [12]. One may assume that in the alloys presented in this study, Si has a similar effect

on the formation of the Laves phase. This phenomenon has to be confirmed in future studies by investigation of the microstructure of the alloy Ta-Mo-Cr-Ti-Al with different Si concentrations.

Further, for two phase Cr(Ta)-Cr$_2$Ta alloys it has been reported that the Cr$_2$Ta Laves phase acts as a sink for nitrogen and effectively getters a flux of nitrogen that passes through the scale [30]. If the scale, however, becomes highly permeable to nitrogen and a strong inward diffusion of nitrogen through grain/phase boundaries takes place massive nitridation of the matrix phase between the Laves phase particles may result [31]. The EBSD measurements (see Fig. 8) on the alloy Ta-Mo-Cr-Ti-Al after 6 h of exposure to 1000 °C confirm this hypothesis by exhibiting preferential formation of metastable CrN (see table 3). Apparently, the thermodynamic equilibrium is not reached after 6h of oxidation. However, after 48h of exposure, the stable modification of the Cr-nitride, Cr$_2$N, was detected (see Fig. 5).

Table 2. Standard free energy of formation of oxides at 1000 °C.

Oxide	Cr$_2$O$_3$	Ta$_2$O$_5$	TiO$_2$ (rutile)	Al$_2$O$_3$	MoO$_3$
ΔG^0[kJ/mole O$_2$]	-538	-598	-713	-853	-293

Table 3. Standard free energy of formation of nitrides at 1000 °C.

Nitrides	Cr$_2$N	CrN	Ti$_2$N	TiN	TaN	Ta$_2$N	AlN
ΔG^0[kJ/mole N$_2$]	-64	-41	-499	-435	-302	-323	-367

With regard to the high temperature oxidation resistance, this study shows the high potential of refractory HEAs. Although these results suggest that the addition of Si had no direct beneficial effect on the oxidation resistance, the effect of Si might be rather complex and should be investigated further. Therefore, the following investigations will be made and will be published in our future works:

1) The effect of nitridation on the high temperature corrosion is rather strong and should be suppressed by using Ar-20 vol.% O_2 atmosphere for the future oxidation experiments. In addition, several discontinuous experiments with short exposure times will be made to investigate the transient oxidation behavior.

2) The volume fraction and size of the Laves phase will be increased by additional heat treatment and the effect on the high temperature oxidation behavior in Ar-$20O_2$ atmosphere will be investigated.

3) Besides, the volume fraction of the Laves phase will be decreased by variation of the Cr and Ta concentrations, too. Thereby, the effect of the chemical composition and the microstructure on the high temperature oxidation behavior under Ar-20 vol.% O_2 atmosphere should be investigated.

Summary

In this study the effect of 1 at.% Si addition on the microstructure and high temperature oxidation resistance of the novel refractory alloy Ta-Mo-Cr-Ti-Al was investigated. The following findings can be summarized:

1.) Both alloys consist of a bcc/B2 matrix with Cr_2Ta Laves phase particles of the three modifications, i.e. cubic C15, hexagonal C14 and C36, at the grain

boundaries and inside the grains. The addition of Si clearly increases the volume fraction and size of the Cr_2Ta Laves phase particles.

2.) The oxidation resistance of both alloys between 900°C and 1100 °C in air is on the level of chromia forming alloys due to the formation of protective chromia-rich and alumina-rich scales. In addition, TiO_2, Ta_2O_5 or $CrTaO_4$ mixed oxide layers were found. The slightly higher oxidation rates were observed for the alloy Ta-Mo-Cr-Ti-Al-1Si as compared to the Si-free HEA. This is explained by the marginally thicker oxide scales and notably more pronounced internal corrosion attacks identified for the Si-containing alloy.

3.) The phase boundaries between the Laves phase and the bcc/B2 matrix serve as preferred diffusion paths for the oxygen and nitrogen ingress. The internal corrosion process along the phase boundaries is more pronounced along the bigger Laves phase particles of Ta-Mo-Cr-Ti-Al-1Si and is probably the main reason for the deleterious effect of 1at.% Si addition on the high temperature oxidation resistance of the alloy Ta-Mo-Cr-Ti-Al-1Si.

References

[1] Yeh J, Chen LY, Lin SJ, et al. High entropy alloys – A new era of exploitation. Mater Sci Forum. 2007;560:1-9.

[2] Senkov ON, Woodward C, Miracle DB. Microstructure and properties of aluminum-containing refractory high entropy alloys. JOM-J Min Met Mat S. 2014; 66:2030-2042.

[3] Senkov ON, Senkova SV, Dimiduk DM, et al. Oxidation behavior of a refractory NbCrMo0.5Ta0.5TiZr alloy. J Mater Sci. 2012;47:6522-6534.

[4] Gao M, Yeh JW, Liaw PK, et al. High entropy alloys-fundamentals and applications. Springer International Publishing Switzerland, 2016.

[5] Miracle DB, Senkov ON. A critical review of high entropy alloys and related concepts. Acta Mater. 2017;122:448-511.

[6] Senkov ON, Senkova SV, Woodward C, et al. Low-density, refractory multi-principal element alloys of the Cr–Nb–Ti–V–Zr system: Microstructure and phase analysis. Acta Mater. 2013;61:1545-1557.

[7] Senkov ON, Woodward C, Miracle DB. Microstructure and properties of aluminum-containing refractory high entropy alloys. JOM-J Min Met Mat S.2014;66:2030-2042.

[8] Senkov ON, Isheim D, Seidman DN, et al. Development of a refractory high entropy superalloy. Entropy. 2016;16:1-13.

[9] Chen H, Kauffman A, Gorr B, et al. Microstructure and mechanical properties at elevated temperatures of a new Al-containing refractory high entropy alloy Nb-Mo-Cr-Ti-Al. J Alloy Compd. 2015;661:206-215.

[10] Senkov ON, Senkova SV, Dimiduk DM, et al. Oxidation behavior of a refractory NbCrMo0.5Ta0.5TiZr alloy. J Mater Sci. 2012;47:6522-6534.

[11] Gorr B, Mueller F, Christ H-J, et al. High temperature oxidation behavior of an equimolar refractory metal-based alloy 20Nb20Mo20Cr20Ti20Al with and without Si addition, J Alloy Compd. 2016;688:468-477.

[12] Bhowmik A, Pang HT, Edmonds IM, et al. Effect of silicon additions on the high temperature oxidation behaviour of $Cr–Cr_2Ta$ alloys. Intermetallics. 2013;32:373-383.

[13] Scott FH, Gabriel GJ, Wei FI, et al. The development of silicon-containing oxides during the oxidation of iron-chromium-base alloys. Mater Corros. 1987;38:521-531.

[14] Evans HE, Hilton DA, Holm RA, et al. Influence of silicon additions on the oxidation resistance of a stainless steel. Oxid Met. 1983;19:1-12.

[15] Jones DE and Stringer J. The effect of small amounts of silicon on the oxidation of high-purity Co-25 wt. % Cr at elevated temperatures. Oxid Met.1975;9:409-413.

[16] Heilmaier M, Krüger M, Saage H, et al. Metallic materials for structural applications beyond nickel-based superalloys, JOM-J Min Met Mat S. 2009;61:61-67.

[17] Li B and Gleeson B. Effects of silicon on the oxidation behavior of Ni-base chromia-forming alloys. Oxid Met. 2006;65:101-122.

[18] Radavich JF. Effect of silicon on high temperature oxidation of stainless steels. Corrosion. 1959;15:613-617.

[19] Durham R, Gleeson B, Young DJ. Silicon contamination effects in the oxidation of carbide-containing cobalt-chromium alloys, Mater Corros. 1998;49:855-863.

[20] Wang S, Wu Y, Gesmundo F, et al. The effect of Si additions on the high-temperature oxidation of a ternary Ni–10Cr–4Al alloy in 1 atm O_2 at 900°C–1000 °C. Oxid Met. 2008;69:299-315.

[21] Cahn RW, Haasen P, Kramer EJ. Materials science and technology; materials corrosion and environmental degradation, Part I and II. Weinheim: Wiley-VCH; 2000.

[22] Klopp WD. Recent Developments in Chromium and Chromium Alloys. NASA Technical Memorandum (US);1969. (NASA TM X-1867).

[23] Massard P, Bernier JC, Michel A. Effet Jahn-Teller dans le système Ta_2CrO_6-$TaCrO_4$. J Solid State Chem. 1972;4:269-274.

[24] Tena MA, Llusar M, Badenes JA, et al. Influence of precursors on formation of TiO_2-$CrTaO_4$ rutile solid solutions. Brit Ceram T. 2000;99:219-224.

[25] Joy JE, Nag A, Gopalakrishnan J, et al. $FeTiTaO_6$: A lead-free relaxor ferroelectric based on the rutile structure. Adv Mater. 2008;20:1348-1352.

[26] Murray MJ, Sanders JV. Close-packed structures of spheres of two different sizes II. The packing density of likely arrangements. Philosophical Magazine A. 1980;42:721-740.

[27] Brady MP, Smialek JL, Smith J, et al. The role of Cr in promoting protective alumina scale formation by y-based Ti-Al-Cr alloys-Part I. Acta Mater.1997;45:2357-2369.

[28] Brady MP, Smialek JL, Smith J, et al. The role of Cr in promoting protective alumina scale formation by y-based Ti-Al-Cr alloys-Part II. Acta Mater.1997;45:2371-2382.

[29] Statham PJ. Limitations to accuracy in extracting characteristic line intensities from X-ray spectra, J Res Natl Inst Stand Technol.2002;107:531-546.

[30] Brady MP, Zhu JH, Liu CT, et al. Oxidation resistance and mechanical properties of Laves phase reinforced Cr in-situ composites. Intermetallics. 2000;8:1119-1129.

[31] Anton DL, Shah DM, Duhl DN, et al. Selecting high-temperature structural intermetallic compounds: The engineering approach. JOM-J Min Met Mat S. 1989;41:12-17.